APPLICATION OF AN HYBRID OPTIMIZATION APPROACH IN THE DESIGN OF LONG ENDURANCE AIRFOILS

Manas S. Khurana*
*The Sir Lawrence Wackett Aerospace Centre, RMIT University, Australia

Keywords: *Airfoil Design, Direct Numerical Optimization, Artificial Neural Networks*

Abstract

Future Re-Configurable Multi Mission Unmanned Aerial Vehicle (RC-MM-UAV) Design concepts are expected to comprise of morphing wings with mission segment based airfoils. The Direct Numerical Optimization (DNO) methodology for airfoil shape optimization is established. The PARSEC shape function is used for airfoil geometry parameterization, coupled with a low-fidelity solver and Particle Swarm Optimizer (PSO) in the design analysis of a long endurance airfoil.

A single-point airfoil design study through the DNO approach was executed. Results indicate that the methodology is computationally demanding thus, Artificial Neural Networks (ANN) are introduced to address this issue. A relationship between PARSEC airfoil geometry variables as inputs and the equating aerodynamic coefficients as outputs are used in network training and validation. The effect of varying training sample size was evaluated to establish a network with acceptable generalization capabilities. The PSO model is integrated to the ANN model for airfoil design optimization. The hybrid PSO/ANN structure required 38% fewer solver calls in comparison to the direct search approach. The proposed hybrid methodology is applicable for future multi-point airfoil design optimizations.

1 Introduction

The growth of unmanned technology has led to major research and development efforts in the aerospace industry. The potential of these aerial platforms has been widely acknowledged worldwide both on civil and military fronts. The designs of UAVs to-date have been uni-mission and considering the envisaged missions in future, a single mission design concept is neither operationally, nor cost effective. A multi-mission aerial platform is identified as a viable alternative.

The Sir Lawrence Wackett Aerospace Centre pioneered a conceptual design of Re-Configurable Multi-Mission Unmanned Aerial Vehicle (RC-MM-UAV) for futuristic civil and military operational needs. Uni mission UAVs presently are under various stages of design, development and trials as an alternative over manned systems to address dull, dirty and dangerous missions. Though uni-mission designs address a certain section of the requirements, the performance is limited; in regards to range/endurance and speeds. A RC-MM-UAV concept will encompass long endurance/range requirements of Intelligence, Surveillance and Reconnaissance (ISR) and the flexibility of speed for Suppression of Enemy Air Defence (SEAD) sorties in its mission profile – a typical futuristic operational scenario. Multi-Mission profile requires variations in speeds, altitude of operation and maneuverability to address disparate performance requirements.

A detail market survey identified the requirement of a Tier of UAVs based on future operational requirements (Table 1) [2]. The Australian program on UAV acquisition covers the request of a High-Altitude Long Endurance UAV for Reconnaissance and Surveillance, thus the development and introduction of an intelligent UAV platform is identified as a key operational asset. The re-configurable modular

concept of wings and payload consisted of disparate mission package. High to medium altitude long endurance consisting of 25-42 hour mission profiles with range in excess of 4,000 nm at Mach numbers 0.32-0.60 was established.

To address the disparate performance requirements of a multi-role platform, an adaptive airfoil shape is identified. Namgoong developed a parallel Genetic Algorithm (GA) for multi-objective airfoil design optimisation [3]. Design tradeoffs of low drag and energy requirements for shape morphing were identified for low subsonic to transonic flow conditions [3]. Gallart optimised airfoils for specific flight segments thus, a single-point optimisation process was undertaken [4], which does not guarantee optimal performance at other flight conditions [4]. The use of artificial neural networks (ANN) for airfoil design optimisation has been proposed. The technique has been used in the design of single [5] and multi-element airfoils [6], including the design of turbomachinery sections [7] and in the minimization of wind tunnel data for aerodynamic performance evaluation [8].

In this paper, a direct search and an ANN model are used in the design optimisation of a single-point airfoil. The performance of the two models is evaluated and compared to observe the validity of each model is providing a feasible solution. The paper is structured as follows: In section 2, airfoil optimisation structure is defined. The PSO search model is validated in section 3 over a series of analytical functions. In section 4 the direct search method is used for airfoil design. The ANN model is utilised in section 5 and comparison between the two search models provided. Finally, the research findings are summarised and an outline of future studies presented in section 6.

2 Problem Definition

To facilitate the design of morphing airfoils, the Direct Numerical Optimization (DNO) architecture is proposed. The methodology comprises of the following: a) Mathematical shape function to represent potential airfoils; b) Flow solver for aerodynamic computation; and c) Intelligent search agent for overall optimization.

2.1 Airfoil Shape Representation

The conformal mapping approach [9] including several mathematical shape functions through the analytical shape representation were examined including the Hicks-Henne bump functions, Legendre, Wagner, Bernstein and NACA normal modes [10-12]. These methods are restricted since the design variables have limited correlation to airfoil geometry parameters. Thus, the application of geometrical constraints for an optimisation run becomes an issue. The PARSEC shape function [13] was implemented in the design optimisation to address this issue. A qualitative analysis through the use of Self-Organising Maps was undertaken to establish a relationship between the PARSEC variables and its effect on airfoil geometry and aerodynamics [14]. The study showed that each variable provides one-to-one geometrical control up to an identified threshold. Aerodynamically, parameters that influence the lift-to-drag ratio, a key requirement in the design of long endurance airfoils, were further identified [14].

2.2 Flow Solver

The second part of the DNO process, involves selecting and validating a computational flow solver. Solution accuracy is enhanced with high-fidelity solvers, at the expense of execution time. The use of Computational Fluid Dynamics (CFD), coupled with parallel processing is proposed to address the issue of solution accuracy and solver convergence time. The NASA LS(1)0417Mod airfoil [15] was used as a case study in the validation process. The results showed that a Reynolds Average Navier Stokes (RANS) model, with a two-equation turbulence model is capable of providing accurate results. The boundary layer tripping point was obtained from experimental data [15] and manually implemented through the development of multi-zonal fluid grid, duplicating regions of laminar and turbulent flows. Comparison between computational and experimental results showed

a lift and drag variance of 3% & 4% respectively, over a linear angle-of-attack range of -1° to 12°.

During preliminary design stages, panel method solvers are proposed due to rapid solution execution. Development of evolutionary programming techniques including neural network methodologies, require extensive test set-up and validation. Low fidelity solvers are ideal for such scenarios. As a result, a series of test simulations involving the integration of the previously identified DNO components can be executed to validate the set-up of the proposed architecture, with acceptable computation time.

2.3 Optimisation Model

The use of evolutionary programming techniques have been extensively used for single and multi objective airfoil shape optimization [5, 16-21]. Gallart examined three gradient-based methods for airfoil drag minimization at a fixed lift coefficient [4]. A sequential quadratic programming technique provided an optimal solution with the lowest number of design iterations [4]. Holst et. al, executed a single objective transonic airfoil design optimization analysis [22]. A genetic algorithm approach was robust, but computationally cumbersome. Thus, the use of gradient methods for single-objective problems was recommended [22].

In this paper, a single-objective, long endurance airfoil, is optimized using a swarm approach. A neural network model is then developed, validated and coupled with PSO for airfoil design optimization. The two techniques are compared to establish the design merits of the two approaches for single-objective designs. The performance of neural networks is of great interest in the context of this research due to the potential computational time benefits on offer.

3 Particle Swarm Optimiser Validation

The search capabilities of the PSO algorithm are verified over a series of benchmark functions, to determine the sensitivity of the model for convergence. SOMs are used to qualitatively show the results of the validation process. The maps illustrate the relationship between variables that control the search process, and its effect on convergence for the proposed test functions. From the maps, the required model set-up which offers robust convergence across the testing envelope can be established. The results of the validation process can then be applied in the proposed design exercise.

The PSO algorithm has evolved with the aim of implementing a robust model that is applicable across various optimization problems [1, 23-25]. The two variants tested in this study include a) Standard-PSO (SPSO) algorithm [24] and; b) Adaptive Inertia Weight (APSO) [1] model (Table 1) which was introduced to add greater search flexibility in comparison to the SPSO algorithm. Both variants are similar in operation, with the exception of calculating the inertia weight, which is modified in the APSO scheme (Table 1).

3.1 Test Functions

The Rosenbrock and Schwefel functions (Eq. 2-3) are used in the validation process. The objective function (Eq. 1) is defined as locating the minimum of the two proposed functions, through the PSO and APSO model (Table 1).

$$\text{Objective Function: } f(x)_{min} \tag{1}$$

Rosenbrock Function:

$$f(x) = \sum_{i=1}^{n-1} [100(x_i^2 - x_{i+1})^2 + (x_i - 1)^2] \tag{2}$$

Schwefel Function:

$$f(x) = 418.9829n - \sum_{i=1}^{n} (x_i \sin\sqrt{|x_i|}) \tag{3}$$

Validation Results

A series of SOM charts are used to represent the results of the validation process. Figure 1 shows the fitness convergence for SPSO (Fig. 1b) and APSO (Fig. 1c), with variations in V_{max} (Fig. 1a) as a percentage of search domain size and solution dimension space, D (Table 2).

The SOM charts (Fig. 1a-c) indicate that low velocity equates to low fitness for both

Table 1. Particle Swarm Optimizer: Model Variants for Validation

PSO Model	SPSO	APSO[1]
Scaling Factors Cognitive & Social (c_1 & c_2)	$c_1 = 2$ $c_2 = 2$	$c_1 = 2$ $c_2 = 2$
Swarm Population (m)	20,40 & 80	20,40 & 80
Number of Dimensions	10,20 & 30	10,20 & 30
Maximum Iterations	1000,1500 & 2000	1000,1500 & 2000
Inertia Weight (w)	$w = \frac{2}{\left\|2-\varphi-\sqrt{\varphi^2-4\varphi}\right\|}$; where $\varphi = c_1 + c_2 = 4$	$ISA_{ij} = \frac{\left\|x_{ij} - p_{ij}\right\|}{\left\|p_{ij} - p_{gj}\right\| + \varepsilon}$ $w_{ij} = 1 - \alpha\left(\frac{1}{1+e^{-ISA_{ij}}}\right)$; where $\alpha = 0.3$
Maximum Velocity (V_{max})	0.1 – 10% of $\lambda_{1\max},\ldots,\lambda_{n\max}$	0.1 – 10% of $\lambda_{1\max},\ldots,\lambda_{n\max}$

SPSO and APSO. This is evident across the test domain, where an increase in D, equates to an increase in fitness. Slow moving particles settle into the global minimum in comparison to faster moving agents that skip key areas of interest. Thus, the particles must navigate about the solution space at slow speeds to assist convergence.

Direct comparison between SPSO and APSO (Fig. 1b-c) indicates that the APSO provides superior convergence across the evaluated testing domain in comparison to the SPSO model (Fig. 1b). The SPSO indicates greater 'hot' regions in red referring to higher fitness with the APSO covering larger 'cold' regions in dark blue thus, indicating that the APSO map has much lower fitness. Comparison between SPSO and APSO (Fig. 1b-c) confirms that a linear decreasing inertia weight, where a global search process is encouraged at the start of the search phase and local during the later stages, provides good solution convergence. A fixed w value, experiences convergence difficulties, since the search pattern or balance between global and local search abilities is constant through out the search phase.

The relationship between particle population (m = 20, 40, 80) and velocity as a function of fitness is represented in Figure 2 for the Rosenbrock model. Higher particle population (m = 80), with the velocity restricted to approximately 0.1% of computational domain, indicates low fitness. With fewer particles (m = 20), at a velocity of 1.0% of $\lambda_{1\max},\ldots,\lambda_{n\max}$, larger fitness is observed (Fig. 2). From this test, it is evident that a larger particle population size assists solution convergence.

The fitness presented here is further compared with the findings reported by Z. Qin et al.[1] with their AIWPSO model [1]. Essentially the APSO used in this study is the model developed by Z. Qin et al. [1] with the exception being in the treatment of the maximum velocity. Essentially Z. Qin et al.[1] fixed V_{max} to equal the maximum distance of each dimension [1]. In this study, the effect of varying V_{max} for both models (Table 1) on solution convergence was evaluated. Table 2 shows fitness comparisons between the SPSO, APSO and Z. Qin et al.[1] AIWPSO model, with the data taken directly from the literature [1]. The SPSO and APSO data in table 2, equates to a velocity threshold of 0.1% of $\lambda_{1\max},\ldots,\lambda_{n\max}$, as this condition was proven to be most effective in Figures 1-2. Comparing the SPSO with AIWPSO model, the SPSO model yields lower fitness. Thus, the benefits of a linearly decreasing inertia weight, in the AIWPSO model does not provide the expected search benefits, as this is counteracted by the higher particle velocity. The SPSO model, which has a fixed inertia weight scheme at lower velocities, outperforms a model with an adaptive inertia weight with higher velocities. Thus the importance of correctly setting the velocity on solution convergence is re-enforced.

Table 2. Rosenbrock Function: Fitness Evaluation Comparison through different PSO Model

Population Size	Dim	Max. Iteration	SPSO	APSO	AIWPSO[1]
20	10	1000	34.4393	17.1394	48.6378
	20	1500	92.4618	17.3522	115.1627
	30	2000	156.8884	19.1374	218.9012
40	10	1000	18.0475	17.2192	24.5149
	20	1500	85.2453	16.7663	60.0686
	30	2000	129.5636	18.8235	128.7677
80	10	1000	13.2744	17.8872	19.2232
	20	1500	79.2820	17.9988	52.8523
	30	2000	100.9905	18.3088	149.4491

The simulation presented in the analysis of the Rosenbrock function, was repeated for the Schwefel model. The function differs from the Rosenbrock, as the design space includes many local minima. Similar results are observed, with a velocity in the range of 0.1% of $\lambda_{1\max},\ldots,\lambda_{n\max}$, providing the lowest fitness. As expected, superior convergence is observed with an increase in particle population size.

4 Direct Search Approach for Single-Point Airfoil Optimisation

Typical single-to-multi objective airfoil optimisation functions, take the following mathematical form:

$$f = \frac{1}{\sum_{i=1}^{q} \frac{C_d(\alpha_i, \mathrm{Re}_i, M_i)}{C_l(\alpha_i, \mathrm{Re}_i, M_i)}} \quad (4)$$

Where:

q = Operating Condition
C_d = Drag Coefficient
C_l = Lift Coefficient
α = Angle - of - Attack
Re = Reynolds Number
M = Mach Number

The specified geometrical and aerodynamic constraints are related and used to define the optimisation problem as:

$$\min f_i(x)$$

$$\text{Subject to: } \begin{matrix} a_{ij}(x) = ad_{ij}, & ij = 1,2,\ldots q \\ g_{ik}(x) = c_{1ik} < t < c_{2ik} & ik = 1,2,\ldots q \end{matrix}$$

where:

f_i = Optimisation of Objective Function at an Operating Condition
$x = [x_1, x_2, \ldots x_{10}]$; Vector of PARSEC Design Variables
$a_{ij}(x)$ = Equality Aerodynamic Constraint at Operating Condition i = (i.e. Fixed C_l, ad_{ij})
q = Number of Constraints
ik = Inequality Geometrical Constraint t, at Operating Condition i

In this paper, a single-objective, constrained optimisation run with the aim of minimising drag at fixed lift coefficient and steady cruise conditions is stipulated (Eq. 5).

$$\begin{aligned} &\min C_d \\ &\text{Subject to: } C_l = 0.4 \\ &\alpha = 2^{\circ} \\ &\mathrm{Re} = 6.0 \times 10^6 \\ &\mathrm{Mach} = 0.32 \\ &0.14 \le t \le 0.24 \end{aligned} \quad (5)$$

Thickness-to-chord constraint for minimum wing volume requirements is specified through PARSEC variables 2 & 5, with the remaining coefficients relaxed, to allow the PSO to explore the best possible combination (Table 3). The PSO adjusts the PARSEC variables with the coordinates integrated into a flow solver for airfoil aerodynamic computation. The coefficients are used to establish the magnitude of the fitness function, with the process operating iteratively until convergence.

4.1 Flow Solver

Low and high fidelity solvers are proposed in the context of this research. The accuracy of the two solvers is disparate. Irrespective of the

computational model integrated, it can model the characteristics of the objective function. Thus, the character of the proposed objective function (Eq. 5) will not change due to the fidelity of the solver. Variations in solution accuracy and total computational time for convergence will be evident. A panel method is initially used in the context of this research. The lower computational costs provide an avenue to test the robustness, flexibility and validity of the proposed search algorithm. With the optimiser fine-tuned, CFD will be used to accurately compute the performance of the airfoil.

The Potential Flow around Airfoils with Boundary Layer Coupled One Way (PABLO), panel method program is used to compute the aerodynamic coefficients [26]. The method uses the Thwaites' equations to model the laminar region and Heads' equations to model the turbulent part of the flow [26]. The onset of flow transition and eventual separation is based on Michel's transition criteria. The total drag coefficient over the lifting surface is analysed using the Squire-Young formula [27].

4.2 Results & Discussion

As PSO is a probabilistic search method, two independent runs were executed to observe solution evolution. The convergence fitness and the final optimal airfoil shapes are presented in Figures 3 & 4 respectively. The two simulations produce different history plots (Fig. 3) with solution fitness magnitude differences between the two runs having a negligible effect on the final aerodynamics (Table 4). Run one convergence requires 56 iterations, with simulation two at 38 generations. With a swarm size of 60 particles, this equates to 3360 and 2280 airfoils that were computed by PABLO respectively over the two runs. Due to the low computational cost of panel method solvers, computation time was not an issue. Integration of Navier-Stokes CFD for similar optimisation runs will be computationally demanding.

Table 4. PSO Execution Results

	Fitness	t/c	C_l	C_d	C_l / C_d
Run 1	6.10×10^{-4}	23.57%	0.40	0.0067	≈ 60
Run 2	6.60×10^{-4}	21.71%	0.40	0.0065	≈ 61

Despite the similar aerodynamic properties (Table 4) of the two shapes (Fig. 4), variances in the coefficient of pressure distribution plots are evident (Fig. 5). The results indicate that a multimodal behavior is present for single-objective airfoil shape optimisation problem, which is also confirmed by Ray [28]. Thus, multiple airfoils exist for the proposed objective function and stricter constraints need to be enforced in order to select a suitable planform. Examination over multiple flight conditions and enforcing aerodynamic constraints including maintaining laminar flow and/or avoiding flow separation must be applied. Due to the presence of multiple solutions, total iteration count for convergence varies as a result (Fig. 3).

The evolution of the PARSEC variables during the search process is examined through a series of box plots (Fig. 6). The ten PARSEC variables are mapped at the start and end of the search process, to observe variable convergence. The Inter-Quartile-Range (IQR) of the initial swarm is larger for all variables with the exception of the leading edge radius and the trailing edge direction coefficient. The IQR at the start of the search process is based on the proposed design variable operating bounds from

Table 3. PARSEC Airfoil Geometrical Constraints

Variable Number	Variable Name	Variable Notation	Lower Bound	Upper Bound
1	Upper Crest Abscissa	X_{UP}	0.30	0.60
2	Upper Crest Ordinate	Y_{UP}	0.07	0.12
3	Upper Crest Curvature	Y_{XXUP}	-1	0.2
4	Lower Crest Abscissa	X_{LOW}	0.20	0.60
5	Lower Crest Ordinate	Y_{LOW}	-0.12	-0.07
6	Lower Crest Curvature	Y_{XXLOW}	0.2	1.20
7	Leading Edge Radius	R_{LE}	0.001	0.04
8	Trailing Edge Ordinate	Y_{TE}	-0.02	0.02
9	Trailing Edge Wedge Angle	β_{TE}	3°	40°
10	Trailing Edge Direction	α_{TE}	-25°	-2°
11	Trailing Edge Thickness	ΔY_{TE}	0	0

Table 3. Thus, the box plots show that the PSO explores all possible variable permutations based on the identified operating range. As the search space narrows towards a global solution, most PARSEC coefficients settle to an optimal value, with a reduction in the final swarm IQR. Due to the multimodal behavior of the objective function, the box plots for the leading edge radius, upper and lower crest curvature and the trailing edge direction indicate that these parameters can take multiple values.

5 Artificial Neural Networks

As the DNO process is computationally inefficient, an ANN methodology is proposed. A trained network, when integrated to a heuristic algorithm can significantly reduce the computation expense of airfoil shape optimization. The proposed network de-couples the solver from the DNO process thus, the swarm search methodology operates directly with the trained network. The foreseen computational benefits of the proposed approach is only plausible if the training airfoil population is less than the number of generations required in a direct search approach as outlined in section 4.2.

5.1 Network Modeling

An ANN structure is introduced (Fig. 7), to develop a relationship between PARSEC shape coefficients and the equating aerodynamic coefficients. Greenman suggests utilizing separate networks for the individual aerodynamic coefficients (C_l, C_d and C_m) [6] to improve network generalization. The corresponding aerodynamic coefficients are established as outputs, at a Reynolds and Mach number of 3.0 million and 0.32 respectively. These conditions simulate the cruise phase of a long endurance sortie for the proposed RC-MM-UAV platform.

5.2 Network Training & Validation

The Bayesian regularization approach by MacKay [29] is used to train the network, to improve system generalization capabilities. Latin Hypercube Sampling (LHS) is implemented to distribute the ten PARSEC variables and ensure an even representation of airfoils across the proposed design space [30]. An example of a LHS output for the leading edge radius and trailing edge point is shown in Figure 8 with a sample size of ten.

A trial-and-error process is undertaken to develop a network by varying the number of hidden layers and neurons within the layers and the activation functions. Training sample size was varied from 800-2300 LHS distributed PARSEC airfoils. Additional planforms, not used in the training process were introduced to monitor network generalization capabilities. System performance is measured by observing training and generalization error with an RMS error of zero between trained and target output data set for convergence. Again, separate networks were developed to model the aerodynamic coefficients. The network development trial-and-error process indicated a training database of 2100 airfoils is required to simulate lift and drag coefficient. Both structures were modeled with two hidden layers, with the lift coefficient architecture consisting of 40 neurons within the two layers and tan-sigmoid transfer functions (Table 5). Drag coefficient required additional ten neurons within the two layers, with log-sigmoid used as the transfer function in the first layer (Table 6). Current research focuses on developing an appropriate model to simulate the moment coefficient.

Table 5. ANN Design Structure for Lift Coefficient

Layer	One	Two	Three (C_l Output)
No. of Neurons	40	40	1
Transfer Function	Tan-Sigmoid	Tan-Sigmoid	Linear

Table 6. ANN Design Structure for Drag Coefficient

Layer	One	Two	Three (C_d Output)
No. of Neurons	50	50	1
Transfer Function	Log-Sigmoid	Tan-Sigmoid	Linear

The effect of varying network input population size from 800-2300 planforms was

evaluated. Training and generalization RMS error for the lift coefficient based on the structure presented in Table 5 was examined (Fig. 9a-c). A network with 800 airfoils shows a steady training and validation error over an extended run. A difference of approximately five percent, between actual and network simulated lift coefficients, for a training RMS error of 1.2×10^{-7} was computed. A higher validation RMS error in comparison to training miss-match, together with a steady error run, it is apparent that the network requires further modifications. With no changes to the network architecture (Table 5), airfoil training size was increased to 2100 sections (Fig. 9b). The training residual in this case decreases to zero, with the validation RMS error at $\approx1\times10^{-8}$. Comparison of actual and simulated lift coefficients for the validation set, showed variances of less than one percent between the two data sets. The validation RMS continues to decline during training progression and with acceptable tolerances between actual and simulated lift data, a valid network is developed. A model with 2300 airfoils in Figure 9c indicates an over-fitting trait. The training error remains low as expected, but the network fails to generalize over new input data. A validation RMS error at convergence is $\approx1.2\times10^{-1}$. As a result, differences between actual and simulated lift coefficients reveal errors in excess of 10%-20%. Together with a steady increase in the validation error during training, the network exhibits over-fitting properties.

5.2 Coupling of PSO with ANN for Single-Point Airfoil Optimisation

The single-objective constrained optimisation run from section 4 is presented with the use of a hybrid technique. The PSO model adjusts the PARSEC variables as inputs within the neural network. The network outputs the aerodynamic coefficients of lift and drag and the solution fitness is evaluated. The process operates iteratively until convergence based on the objective function (Eq. 5).

The final optimal shape has an approximate thickness-to-chord ratio of 20% (Fig. 10), with a lift coefficient of 0.40 according to defined flight requirement from equation 5 (Table 7). In general the final results obtained with the hybrid technique, are similar to the analysis presented in table 4, through the direct search approach.

Table 7. PSO / ANN Execution Results

	Fitness	t/c	C_l	C_d	C_l / C_d
ANN / PSO	5.60×10^{-4}	19.8	0.40	0.0066	≈ 61

The fitness of the converged solution is slightly less than the magnitude obtained through the DNO approach (Table 4). This has a negligible effect on the aerodynamics of the final solution (Table 4 & 7). The hybrid approach converged at 223 iterations, which is considerably greater than the direct PSO approach. This is attributed to the differences in the termination criteria set within the two search models. In the direct approach, a conservative termination criterion, with fitness of all the particles to be within 0.05 of each other was set. In the neural net / PSO approach this criteria was extended to 0.005. The aerodynamics of the final solution remains unchanged despite the enforcement of a stricter termination criterion. In the hybrid approach, the overall best solution has been established at iteration 127. The defined termination criterion is such that the relative fitness of all the particles within the swarm is not 0.005 at this stage. As a result, the optimizer continues to execute until all the particles are within this range. Consequently, the fitness of the optimal solution within the swarm remains constant from epoch 127 to the end of the search phase (Fig. 11). This suggests that a magnitude of 0.005 can be relaxed for future analysis.

The results presented here show the benefits of the PSO / ANN approach. The hybrid methodology required 38% and 8% fewer airfoil solver executions, in comparison to the direct search approach from runs 1 and 2 respectively. The aerodynamics of the final solution between the two methods was negligible thus, further illustrating the benefits of this approach. The final optimal shapes in the three simulations (two from the direct approach + one from the hybrid technique) are unique but share similar aerodynamic performance. The

hybrid approach has further verified the presence of a multimodal design space for single-point airfoil designs.

The true benefits of this approach will be apparent, when high-fidelity solvers are introduced within the design optimization framework. It was seen that a neural network requires fewer airfoil samples thus, reduced solver time in comparison to a direct search approach. Navier-Stokes models, when implemented for network training and integrated to a PSO algorithm, will provide accurate aerodynamic coefficients for airfoil shape optimization, with reduced computational load.

6 Conclusion and Future Research

The DNO approach for airfoil design and analysis was introduced. The PSO model was validated for application in airfoil design. Two benchmark functions were used in the validation process. The effect of varying particle population and velocity across multiple dimensions, on solution convergence was examined. The results were mapped onto a series of SOM charts, which showed that the adaptive inertia weight model was superior in comparison to a standard PSO algorithm. Large particle population with low velocities provides acceptable convergence in comparison to an optimization run with fewer particles navigating at faster speeds. Current research focuses on developing an adaptive inertia velocity function, similar to the inertial weight model, to adapt the speed of the particles through a PSO run. This has the potential of providing greater solution agreement with fewer design iterations.

The direct search method was used for a single-point airfoil optimisation. Series of aerodynamic and geometrical constraints were applied. A single-point optimisation run is characterised by a multi-modal solution space. The need to enforce stricter aerodynamic constraints and a multi-objective function is required to address this issue. Panel method calculations showed that a direct optimisation run is computationally demanding. Integration of high-fidelity solvers will result in computationally inefficient optimisation architecture.

An ANN methodology within the overall DNO framework was introduced to address the issue of high computational cost. The PARSEC design variables were used as inputs with the equating aerodynamic coefficients as outputs. A detail network development study was undertaken through variations in training sample size and altering network set-up. A model with two hidden layers comprising of 40 and 50 neurons for lift and drag respectively was required. Together with a training sample size of 2100 airfoils, the network simulated lift and drag to one percent of actual solver solution. Current research focuses on developing a network to simulate the moment coefficient. The hybrid methodology was then used in the design of an airfoil; repeat of the analysis performed through the direct search approach. Comparison of results between the hybrid approach and the two stand-alone PSO simulations indicated computational saving in the range of 8% - 38%. Future research focuses on performing a multi-point airfoil design analysis. With the introduction of a moment coefficient neural network and Navier-Stokes models, stricter aerodynamic constraints can be imposed, to reduce the multimodal behavior of the search process. The computational resources through the utilization of high-fidelity solvers will benefit from the proposed hybrid search methodology.

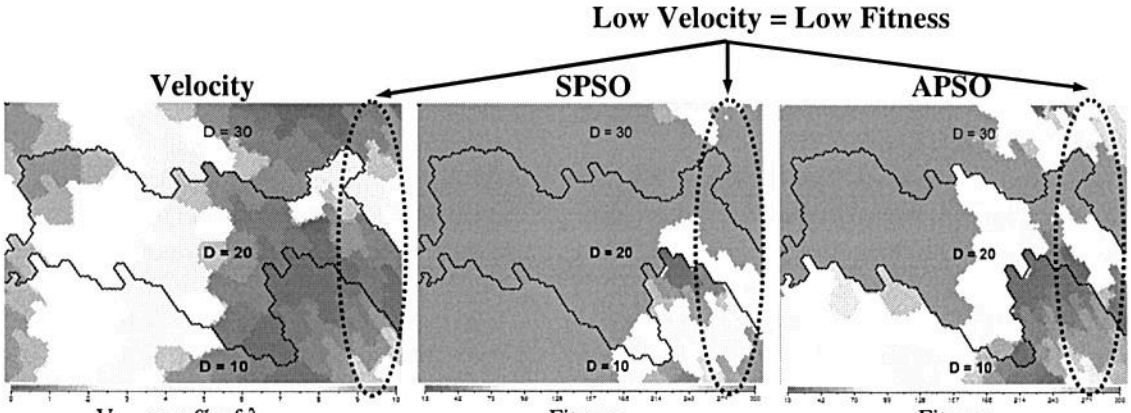

Fig. 1 Rosenbrock Function Convergence: SOM Visualization

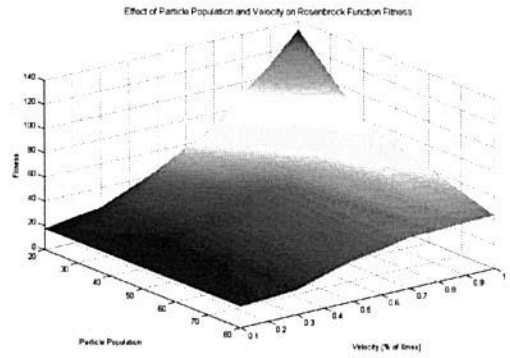

Fig. 2 Rosenbrock Function: Effect of Varying Particle Population & Velocity on Fitness

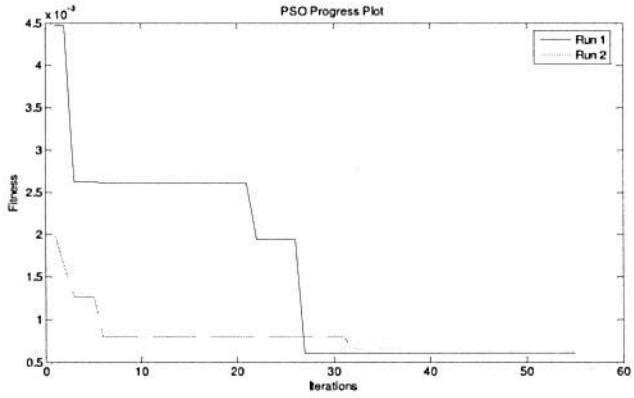

Fig. 3 Convergence Plot

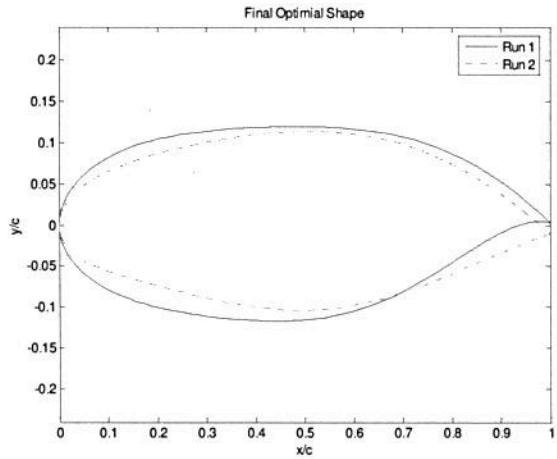

Fig. 4 Final Optimal Airfoil Shapes

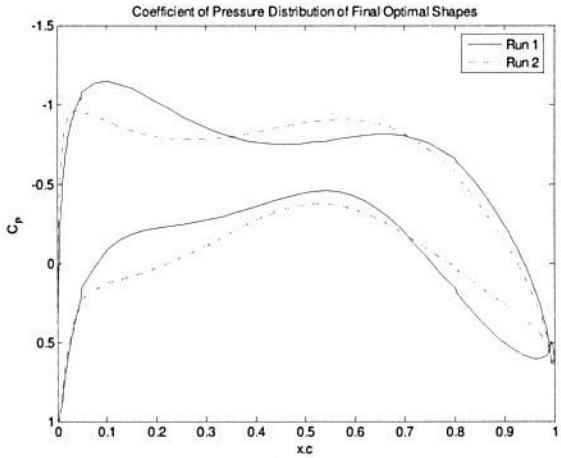

Fig. 5 Optimal Airfoil Shapes Coefficient of Pressure

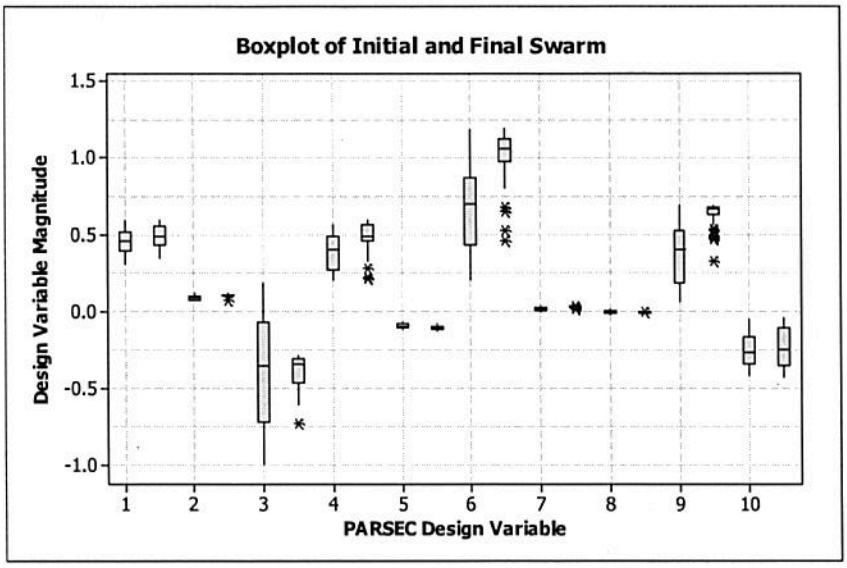

Fig.6 Box Plot of Initial and Final Swarm (Run 2)

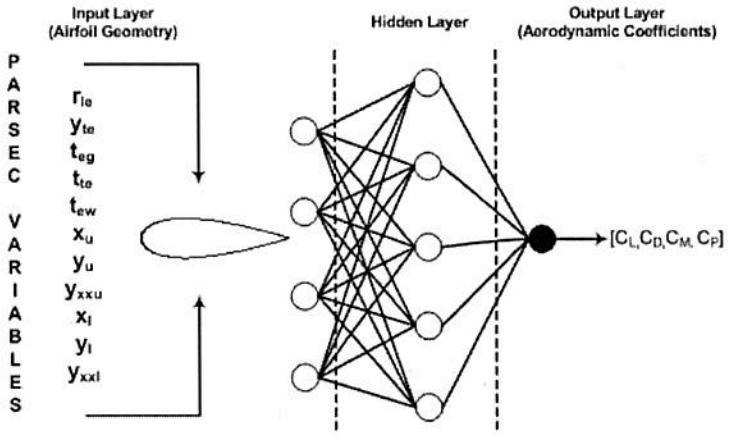

Fig. 7 Proposed Artificial Neural Networks Structure

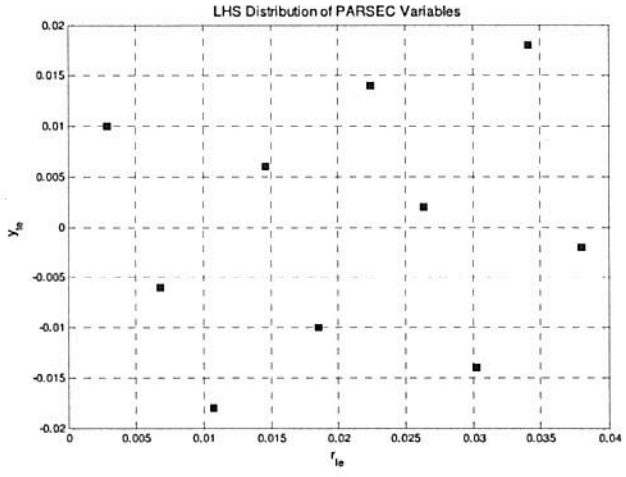

Fig. 8 Latin Hypercube Sampling of PARSEC Variable y_{te} and r_{le}

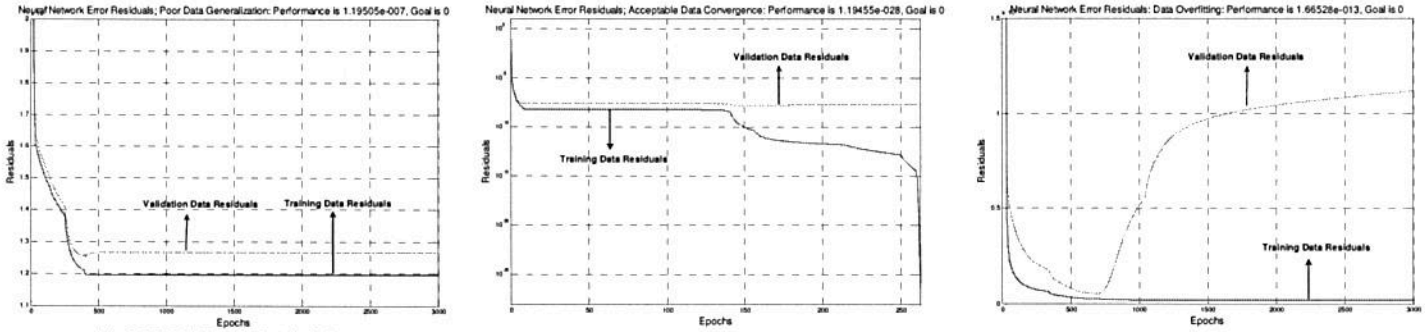

(a) 800 PARSEC Airfoils (b) 2100 PARSEC Airfoils (c) 2400 PARSEC Airfoils

Fig. 9 ANN Lift Coefficients Training Plots

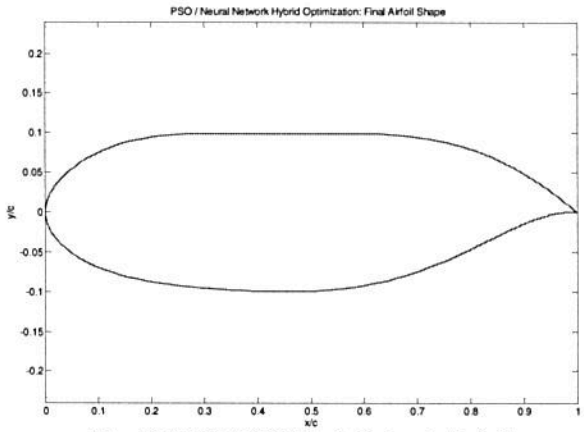

Fig. 10 ANN / PSO Final Optimal Airfoil

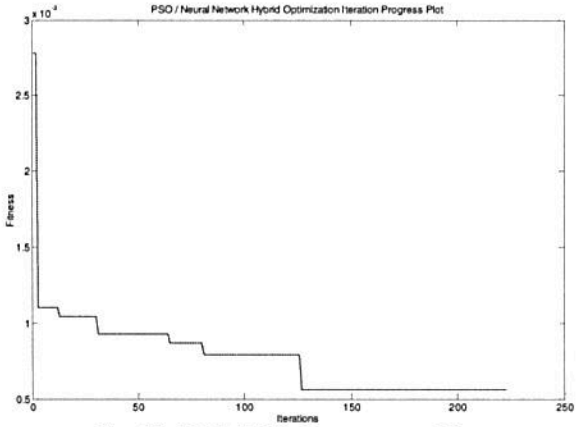

Fig. 11 ANN / PSO Convergence Plot

References

[1] Qin, Z., et al., 2006, 'Adaptive Inertia Weight Particle Swarm Optimization,' *Proceedings of the ICAISC 2006,* Springer-Verlag Berlin Heidelberg pp. 450-459

[2] Wong, D. K. C., 1997, "Aerospace Industry Opportunities in Australia - Unmanned Aerial Vehicles (UAVs) - Are They Ready This Time? Are We?," University of Sydney, NSW 26 November

[3] Namgoong, H., 2005, 'Airfoil Optimization of Morphing Aircraft', PhD thesis, Purdue, Indiana.

[4] Gallart, M. S., 2002, 'Development of a Design Tool for Aerodynamic Shape Optimization of Airfoils', Master of Applied Science thesis, University of Victoria.

[5] Hacioglu, A., "Fast Evolutionary Algorithm for Airfoil Design via Neural Network," *AIAA Journal*, vol. 45, No. 9, pp. 2196-2202, 2007.

[6] Greenman, R. M. & Roth, K. R., "Minimizing Computational Data Requirements for Multi-Element Airfoils Using Neural Networks," *Journal of Aircraft*, vol. 36, No. 5, pp. 777-784, 1999.

[7] Rai, M. M. & Madavan, N. K., 1998, 'Application of Artificial Neural Networks to the Design of Turbomachinery Airfoils,' *Proceedings of the 36th Aerospace Sciences Meeting & Exhibit, Reno, NV 1998,* AIAA pp.

[8] Ross, J. C., Jorgenson, C. C. & Norgaard, M., 1997, "Reducing Wind Tunnel Data Requirements Using Neural Networks," NASA Technical Memorandum, Moffett Field, CA May 1997

[9] Khurana, M., Sinha, A. & Winarto, H., 2007, 'Multi-Mission Re-Configurable UAV - Airfoil Analysis through Shape Transformation and Computational Fluid Dynamics,' *Proceedings of the Twelfth Australian International Aerospace Congress - Second Australasian Unmanned Air Vehicles Conference 21st March, 2007,* pp. 1-22

[10] Khurana, M., Sinha, A. & Winarto, H., 2007, 'Multi-Mission Re-Configurable UAV - Airfoil Shape Parameterisation Study,' *Proceedings of the 22nd International Unmanned Air Vehicle Systems Conference, Bristol 16th-18th April, 2007,* pp. 1-15

[11] Khurana, M., Sinha, A. & Winarto, H., 2008, 'Multi Mission Re-Configurable UAV - Airfoil Optimisation through Swarm Approach and Low Fidelity Solver,' *Proceedings of the 23rd Bristol*

International Unmanned Air Vehicle Systems Conference, Bristol, United Kingdom 2008, pp.

[12] Khurana, M., Winarto, H. & Sinha, A., 2008, 'Airfoil Geometry Parameterization through Shape Optimizer and Computational Fluid Dynamics,' *Proceedings of the 46th AIAA Aerospace Sciences Meeting and Exhibit, Reno, Nevada 2008,* American Institute of Aeronautics and Astronautics pp. 18

[13] Sobieczky, H., "Parametric Airfoils and Wings," *Numerical Fluid Dynamics*, vol. 68, 71-88, 1998.

[14] Khurana, M., Winarto, H. & Sinha, A., 2008, 'Application of Swarm Approach and Artificial Neural Networks for Airfoil Shape Optimization,' *Proceedings of the 12th AIAA/ISSMO Multidisciplinary Analysis and Optimisation, Victoria, British Columbia, Canada 2008,* AIAA

[15] McGhee, R. J. & Beasley, W. D., 1981, "Wind-Tunnel Results for a Modified 17-Percent-Thick Low-Speed Airfoil Section," NASA, Virginia, NASA Technical Paper

[16] Barrett, T. R., Bressloff, N. W. & Keane, A. J., "Airfoil Shape Design and Optimization Using Multifidelity Analysis and Embedded Inverse Design," *AIAA Journal*, vol. 44, No. 9, pp. 2051-2060, 2006.

[17] Fuhrmann, H., "Design Optimisation of a Class of Low Reynolds, High Mach Number Airfoils For Use in the Martian Atmosphere," *23rd AIAA Applied Aerodynamics Conference*, 2005.

[18] Hager, J. O., Eyi, S. & Lee, K. D., "Two-Point Transonic Design Using Optimization for Improved Off-Design Performance," *Journal of Aircraft*, vol. 31, No. 5, pp. pp 1143-1147, 1994.

[19] Hua, J., et al., "Optimization of Long-Endurance Airfoils," *21st AIAA Applied Aerodynamics Conference*, pp 1-7, 2003.

[20] Jeong, S., Murayama, M. & Yamamoto, K., "Efficient Optimization Design Method Using Kriging Model," *AIAA Aerospace Sciences Meeting and Exhibit*, vol. 42, No. 2, pp. 413-420, 2004.

[21] Liu, J.-L., "Novel Taguchi-Simulated Annealing Method Applied to Airfoil and Wing Planform Optimization," *Journal of Aircraft*, vol. 43, No. 1, pp. 102-109, 2006.

[22] Holst, T. L. & Pulliam, T. H., 2001, "Aerodynamic Shape Optimization Using a Real-Number-Encoded Genetic Algorithm," NASA, Moffett Field, CA June

[23] Eberhart, R. C. & Shi, Y., "Particle Swarm Optimization: Developments, Application, and Resources," *Congress on Evolutionary Computation CEC2001, IEEE*, vol. 1, 81-86, 2001.

[24] Eberhart, R. C. & Shi, Y., "Comparing Inertia Weights and Constriction Factors in Particle Swarm Optimization," *Congress on Evolutionary Computation*, vol. 1, 84-88, 2000.

[25] Zheng, Y.-l., et al., 2003, 'Empirical Study of Particle Swarm Optimizer with an Increasing Inertia Weight,' *2003,* pp. 221-226

[26] Wauquiez, C., "Potential Flow around Airfoils with Boundary Layer coupled One-way (PABLO)." Stockholm, Sweden: KTH - The Royal Institute of Technology, Department of Aeronautics, 1999.

[27] Katz & Plotkin, 1991, *Low Speed Aerodynamics, from Wing Theory to Panel Methods*. McGraw-Hill Inc.

[28] Ray, T. & Tsai, H. M., "Swarm Algorithm for Single-and Multiobjective Airfoil Design Optimization," *AIAA Journal*, vol. 42, No. No. 2, pp. 366-373, 2004.

[29] MacKay, D. J. C., "Neural Computation: Bayesian Interpolation," *Neural Comput.*, vol. 4, No. 3, pp. 415-447, 1992.

[30] McKay, M. D., Beckman, R. J. & Conover, W. J., "A Comparison of Three Methods for Selection Values of Input Variables in the Analysis of Output From a Computer Code," *Technometrics*, vol. 21, No. 2, pp. 239-245, 1979.

Copyright Statement